







INVESTIGATING MICROARCHITECTURAL CHARACTERISTICS OF WOVEN BONE EXPOSED TO IONIZING RADIATION: COMPARATIVE ANALYSIS OF TWO SEGMENTATION METHODS AND THEIR IMPACT ON TRABECULAR MEASUREMENTS IN AN ANIMAL STUDY

Tássio Edno Atanásio PITORRO^{1,2} , Milena Suemi IRIE¹ , Clara de Oliveira Barbosa BITES¹ , Gabriella Lopes de Rezende BARBOSA³ , Gustavo Davi RABELO⁴ , Priscilla Barbosa Ferreira SOARES¹ 

¹Department of Periodontology and Implantology, Universidade Federal de Uberlândia, Uberlândia, MG, Brazil.

²Department of Dentistry, Zambeze University, Tete, Mozambique.

³Department of Oral Diagnosis, Universidade Federal de Uberlândia, Uberlândia, MG, Brazil.

⁴Department of Dentistry, Universidade Federal de Santa Catarina, Florianópolis, SC, Brazil.

Corresponding author:

Priscilla Barbosa Ferreira Soares
pbfoares@ufu.br

How to cite: PITORRO, T.E.A., et al. Investigating microarchitectural characteristics of woven bone exposed to ionizing radiation: comparative analysis of two segmentation methods and their impact on trabecular measurements in an animal study. *Bioscience Journal*. 2025, **41**, e41003. <https://doi.org/10.14393/BJ-v41n0a2025-75383>

Abstract

The study aimed to evaluate bone formation in surgical defects exposed to ionizing radiation (IR) and to compare two image segmentation methods: manual and standardized delimitation of the region-of-interest (ROI). Bone defects were created in the tibias of Wistar rats using a 2.3 mm trephine. After seven days, the animals were exposed to IR (30 Gy single dose). Two weeks later, the animals were euthanized, and their tibias were scanned using X-ray microtomography. ROI definition was performed by a single operator using two methods: (a) interactive segmentation, where the woven bone was manually outlined within the bone defect region, and (b) a standardized, predefined rectangular ROI. Bone volume fraction (BV/TV), trabecular thickness (Tb.Th), trabecular separation (Tb.Sp), trabecular number (Tb.N), bone surface (BS/BV), and fractal dimension (FD) were assessed for both segmentation methods. Significant differences were observed for BV/TV ($p < 0.001$), Tb.N ($p < 0.001$), and Tb.Sp ($p < 0.001$), but not for Tb.Th ($p = 0.71$), BS/BV ($p = 0.79$), and FD ($p = 0.35$). The manual method was approximately 3.5 times more time-consuming than the predefined ROI method (446.2 ± 49.5 vs 131.2 ± 38.8 s, $p < 0.001$). None of the evaluated parameters showed significant differences when the IR was considered. Within the limitations of this study, the findings indicate that IR does not interfere with the bone repair process when delivered post-surgery. While manual segmentation is more time consuming, it retrieves greater bone volume and reveals differences in trabecular structure, showing more trabeculae number and less trabeculae separation in irradiated bone.

Keywords: Bone. Fractals. X-Ray Microtomography.

1. Introduction

X-ray microtomography, or micro-computed tomography (micro-CT), is widely used to assess bone tissue properties (Nascimento et al. 2019; Su et al. 2024). This nondestructive, high-resolution sectional imaging method enables the identification of microarchitectural aspects crucial for understanding bone remodeling and repair processes, mechanical properties, and susceptibility to disease (Adams et al. 2022; Shim et al. 2022; Beitlitum et al. 2024). By acquiring images from multiple viewing angles around the sample, micro-CT reconstructs three-dimensional (3D) structures at a micrometric scale, providing insights

into 3D geometry and tissue properties (Bouxsein et al. 2010; Clark and Badea 2014; Kim et al. 2021). This methodology provides a relatively short turnaround time and high throughput (Chavez et al. 2021) and shares the same physical principles as clinical computed tomography scanners, but with higher resolution imaging (Clark and Badea 2014; Vársárhelyi et al. 2020). Micro-CT is currently considered the gold standard for quantifying 3D bone microarchitecture in animal models (Bouxsein et al. 2010; Beitlitum et al. 2024). Variables associated with image acquisition, processing, and analysis of micro-CT scans can influence the morphological results obtained from bone samples (Christiansen 2016). One of these variables is the segmentation of the analyzed structures, which is the first step in structural analysis and is critical for accurately quantifying architectural parameters (Buie et al. 2007). Segmentation involves two key steps: defining a region of interest (ROI) and binarizing the image to separate bone from the background. These steps significantly impact the outcomes of micro-CT analyses, including trabecular and cortical bone assessments (Buie et al. 2007; Christiansen 2016).

The microarchitecture of woven bone within the bone-repair region can be assessed using trabecular parameters. Beyond conventional microarchitectural parameters, texture analysis can also be performed using fractal dimension (FD) analysis. This index is directly related to bone spatial distribution and complexity (Irie et al. 2018; de Oliveira Loures et al. 2023). To assess bone tissue properties related to microarchitecture, studies have concentrated on the micro-CT methodology in both animal and human samples, revealing that several steps are necessary to properly assess the architectural parameters of the trabeculae and marrow spaces (Buie et al. 2007; Viguet-Carrin et al. 2010; Irie et al. 2018). However, the influence of segmentation processes and ROI definition prior to binarization on morphometric outcomes remains underexplored.

Radiotherapy (RT) is a common treatment for head and neck cancers (Manem and Taghizadeh-Hesary 2024). Advances in early diagnosis have increased life expectancy among these patients (Sari et al. 2024). However, radiation-induced long-term adverse effects remain a growing concern for physicians (Jiang et al. 2021). Ionizing radiation (IR) can influence woven bone formation, impacting certain microarchitectural parameters while leaving others unaffected (Mendes et al. 2020; Donaubauer et al. 2020). This study aimed to assess differences between manual and predefined standardized ROI segmentation methods applied in micro-CT images for microarchitectural bone analysis. Additionally, the bone repair process following IR exposure was assessed. The null hypothesis posited that the segmentation method would not influence the outcomes of micro-CT analysis, and that IR would not affect the bone repair process.

2. Material and Methods

Animals

This study was approved by the Bioethics Committee for Animal Experimentation (CEUA #045/20) at the Federal University of Uberlândia (Brazil) and adhered to the ARRIVE guidelines and the normative guidelines of the National Council for Animal Control and Experimentation (CONCEA). Twenty-four male Wistar rats, aged three months and weighing 300–350 g, were included. The animals were acclimatized for two weeks before the experimental procedures. Randomization was performed using Random.org (<https://www.random.org>). The animals were housed in groups of four per standard cage with food and water provided ad libitum, under controlled conditions (ambient temperature 22 °C, controlled humidity, and a 12-hour light-dark cycle). A pilot study revealed that the ROI segmentation method affected the results, whereas IR did not. Based on these findings, the total sample size was set at 24 animals, allocated into four groups (n=6): non-irradiated and prefed ROI, non-irradiated and manual ROI, Irradiated and prefed ROI, and irradiated and manual ROI.

Surgical procedure

Animals were anesthetized via intraperitoneal administration of 100 mg/kg ketamine hydrochloride (10%) (Ketamina Agener®; Agener União Ltda, São Paulo, SP, Brazil) with 10 mg/kg of xylazine

hydrochloride (2%) (Rompum® Bayer SA, São Paulo, SP, Brazil). Both animal legs were shaved and cleaned with a 2% chlorhexidine solution (Clorexoral® Biodinâmica, Ibiporã, PR) to prevent infections. Incisions of 3 cm in length were made on the animal legs, and the soft tissue and periosteum were repositioned to expose the proximal regions of the tibias. A bone defect of 2.3 mm diameter was created in the exposed region using a spherical drill (#8) operated at a low-speed straight headpiece and cooled with physiological saline solution. The depth of perforation was limited to the rupture of the cortical bone. Subsequently, the animals received post-surgical care, which included administration of drugs such as tramadol hydrochloride (Tramadol®, Hipolabor, Belo Horizonte, Brazil) twice a day, at a dose of 5 mg/Kg, during three days and pentabiotic (Pentabiotico®, Zoetis Indústria de Produtos Veterinários Ltda, Brazil) at a dose of 24.000 UI/kg, twice, with five day intervals. During the entire postoperative period, the animals were carefully monitored once daily for five days.

Radiotherapy

Seven days after the surgical procedure, 12 animals were randomly assigned to receive external RT, while the remaining 12 underwent RT simulation (sham method). The animals were anesthetized in the same manner as for the surgical procedure. Both legs were positioned laterally and fixed using adhesive tape. A wax bolus with a thickness of 15 mm was positioned over the legs to allow optimal delivery of the radiation dose. The beam was collimated, and irradiation was delivered using a linear accelerator with a direct electron beam of 6 MeV electrons (Varian 600- C®; Varian Medical Systems Inc., Palo Alto, CA, USA). The photons were delivered as a single dose of 30 Gy (dose rate of 400 cGy/min) with a source–skin distance of 60 cm. Irradiation was restricted to the tibial region by using a laser-guided system to define and limit the field (15 × 15), as is usually practiced in patients. Animals exhibiting signs of suffering during the procedure, were excluded from the study and euthanized.

Animal euthanasia and sample processing

Fourteen days after RT (or RT simulation), animals were euthanized via 2.5% thiopental followed by intravenous injection of 19% potassium chloride (Ariston Chemical and Pharmaceutical Industry Ltd. SP, São Paulo, Brazil). Tibias were removed by disarticulation and fixed in 4% paraformaldehyde solution in phosphate-buffered saline for 48 hours.

Micro-CT analyses

Forty-eight tibias (24 from irradiated and 24 from non-irradiated groups) were scanned by a single operator, at an energy of 70 kV and an intensity of 278 µA with an isotropic voxel of 9 µm using an aluminum filter (1 mm thickness) and 180° rotation with an angular increment of 0.4° using micro-CT (Skyscan-1272 X-ray microtomography; Bruker, Kontich, Belgium). NRecon® software (version 1.7.4.2; SkyScan, Bruker, Belgium) was used for sample reconstruction, following the same parameters of smoothing (0), ring artifacts reduction (12), and beam-hardening (40%) for all samples. ROI definition was also performed by a single operator using two different methods (manually defined by the operator's interactive delineation or using a standardized predefined rectangle ROI), culminating in two study factors (IR and ROI definition methods) and four study groups.

Dataviewer® software (version 16.0.0; SkyScan, Bruker, Belgium) was used to select sagittal slices (Figure 1). Top and bottom slice selection by CT-Analyzer® software (version 1.20.8.0; SkyScan, Bruker, Belgium) was performed, including the same number of slices (200) located in the central region of the lesion, for both ROI definition methods. In the manual method, ROI delimitation was performed slice-by-slice following the contours of the newly formed woven bone (Figure 2A). For the method using the predefined-standardized ROI, a rectangular shape was used (2.3x0.5 mm, considering the size of the lesion and the average of rat tibia cortical thickness, respectively) (Figure 2B), fitting it to the center of the bone lesion. Slice-by-slice was checked to correct any possible displacement of the rectangle, since the evaluation approached the periphery of the lesion, its size decreased progressively. In both methods, ROI

delimitation was performed including only lesions located in the cortical region. An interpolation tool was used between the slices, allowing delimitation in a smaller number of slices after careful inspection. A standard threshold (values of upper 255 and lower 62) was applied to ensure that differences between the study groups were inherent to the experiment itself and not to the image processing. The 3D morphometric analysis of the cortical bone lesions was performed. Data related to Bone volume fraction (BV/TV), trabecular thickness (Tb.Th), trabecular separation (Tb.Sp), trabecular number (Tb.N), specific bone surface (BS/BV) and fractal dimension (FD) were obtained. The time consumed for ROI definition of each sample in both groups was carefully counted in seconds.

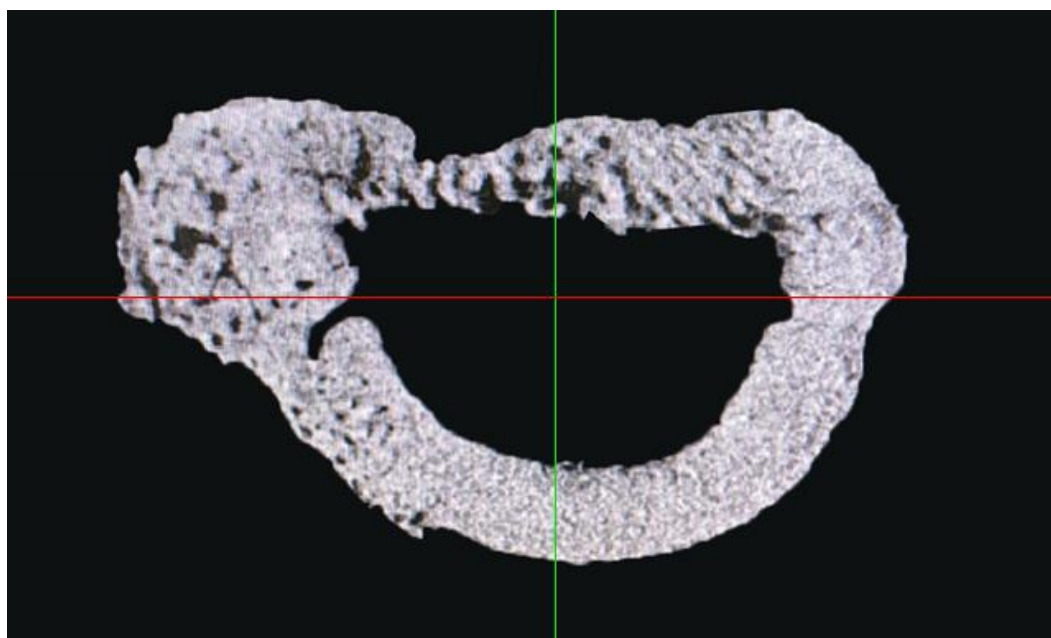


Figure 1. Selection of sagittal section on *Dataviewer*®

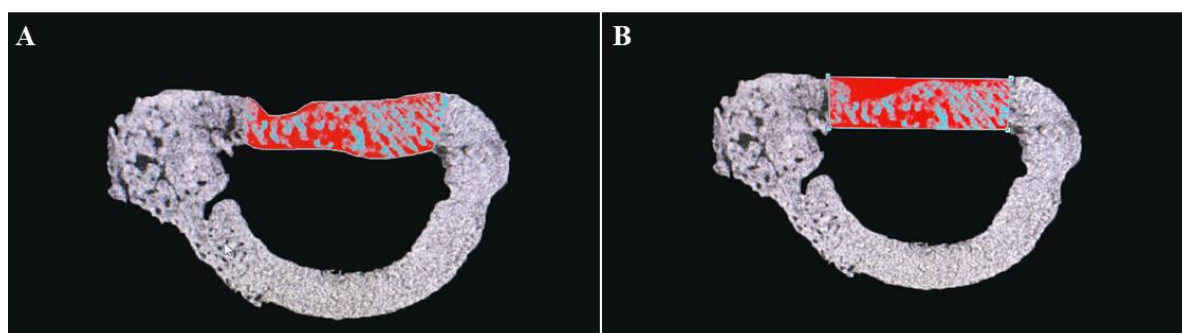


Figure 2. Region of Interest delimitation using *CT-Analyzer*® software. A) manual delimitation; B) predefined delimitation.

Statistical analysis

Statistical analyses were conducted using JAMOV software (version 2.4.1). The normality of data distribution was assessed using the Shapiro–Wilk test, while equality of variance was evaluated with Levene's test. A two-way ANOVA test was employed to analyze the effects of RT and ROI factors. Differences were considered statistically significant at $P < 0.05$. The time consumed for ROI definition (in seconds) for each sample was recorded, and a paired t-test was performed.

3. Results

The means and standard deviations of all evaluated parameters are presented in Table 1. The two-way ANOVA revealed that the ROI definition method significantly influenced the results for BV/TV ($p <$

0.001), Tb.N ($p < 0.001$), and Tb.Sp ($p < 0.001$), but not Tb.Th ($p = 0.71$), BS/BV ($p = 0.79$), and FD ($p = 0.35$). No significant differences were found in the the IR factors for any of the parameters: BV/TV ($p = 0.87$), Tb.N ($p = 0.95$), Tb.Sp ($p = 0.45$), Tb.Th ($p = 0.84$), BS/BV ($p = 0.43$), and FD ($p = 0.31$). A Student's t-test demonstrated that the manual method was approximately 3.5 times more time-consuming (446.2 ± 49.5 s) compared to the predefined-standardized ROI method (131.2 ± 38.8 s) ($p < 0.001$).

Table 1. Differences between two segmentation methods - mean and standard-deviation of BV/TV, Tb.N, Tb.Th, Tb.Sp, BS.BV, and FD parameters.

		Predefined ROI	Manual ROI	p – value	p – value two-way ANOVA
BV/TV	Nlr	59.10 ± 12.50^{Ba}	75.0 ± 7.77^{Aa}	0.002	<0.001
	lr	58.50 ± 12.50^{Ba}	76.50 ± 13.88^{Aa}	<0.001	
Tb.N	Nlr	6.46 ± 1.50^{Aa}	7.86 ± 1.15^{Aa}	0.054	<0.001
	lr	6.13 ± 1.33^{Ba}	8.14 ± 1.19^{Aa}	0.002	
Tb.Th	Nlr	0.09 ± 0.01^{Aa}	0.10 ± 0.02^{Aa}	0.92	0.71
	lr	0.10 ± 0.02^{Aa}	0.10 ± 0.01^{Aa}	0.99	
Tb.Sp	Nlr	0.11 ± 0.03^{Aa}	0.08 ± 0.01^{Aa}	0.10	<0.001
	lr	0.14 ± 0.09^{Aa}	0.06 ± 0.01^{Ba}	0.001	
BS.BV	Nlr	33.0 ± 9.33^{Aa}	31.20 ± 7.24^{Aa}	0.91	0.79
	lr	30.20 ± 5.21^{Aa}	31.0 ± 3.34^{Aa}	0.99	
FD	Nlr	2.34 ± 0.03^{Aa}	2.31 ± 0.04^{Aa}	0.99	0.35
	lr	2.33 ± 0.10^{Aa}	2.13 ± 0.65^{Aa}	0.43	

Different capital letters indicate significant differences within the same row, and different lowercase letters indicate significant differences within the same column.

4. Discussion

The segmentation method of ROI significantly influenced the microtomographic analysis of the three parameters; therefore, the null hypothesis was rejected. The bone volume index associated with trabecular parameters (Tb.Th, Tb.Sp, and Tb.N) is the usual set of variables that should be reported when describing trabecular bone morphology (Bouxsein et al. 2010), also used for woven bone evaluation within the bone repair site. It is essential to measure trabecular parameters because woven bone is the first bone formed during the repair process owing to the rapid deposition of the osteoid matrix, which is replaced by lamellar bone (Bouxsein et al. 2010; Mendes et al. 2020). The present study was based on the results of these parameters and the influence that the ROI delimitation could have on these findings. In addition to conventional microarchitectural parameters, fractal dimension assessment can also be influenced by the ROI definition. The bone spatial complexity evaluation seemed not to be affected by the ROI used, if manually defined individually or by choosing a standardized predefined format for the ROI.

One reason for the difference between the manual and predefined ROI methods lies in the contouring process. In the manual method, an external contour was created around the bone area observed by the operator. In contrast, the predefined method used a rectangular ROI to fill the region corresponding to the lesion; therefore, newly formed bone and surrounding shapes were included. Thus, different proportions of bone volume were considered, particularly for the TV measurements. The BV/TV ratio is considered a critical morphometric parameter for describing the trabecular microstructure (Nascimento et al. 2019). In the present study, this measurement was used to determine the amount of new bone formation within the surgically created bone defects. Our findings revealed that the significant differences in BV/TV with higher values for segmentation using a manually defined ROI can indicate the accuracy of the delineation surrounding the entire bone formed within the lesion, given TV measurements.

The trabecular number and separation values were different only for the woven bone exposed to ionizing radiation during its formation and remodeling process. Using a rectangular ROI with a standardized pattern resulted in fewer trabeculae and more marrow spaces. Two factors should be carefully considered based on these results: 1) irradiation during the bone formation process interferes with bone mineralization; therefore, the identification of structures in the binarized image could be influenced by this

condition. The trabeculae number parameter was only different because the analyzed woven bone had not yet been remodeled to a more advanced stage of maturation. It could be expected that the amount of woven bone would be higher than that of lamellar mature bone if the repair process was not affected by radiation. Another study from our group (Mendes et al. 2020) revealed findings that support this inference, as the woven bone subjected to IR was found to arrest the bone repair process, characterized by morphological changes in the trabecular arrangement of the newly formed bone, together with alterations in the osteocyte characteristics and collagen arrangement; 2) Trabecular separation accounted for not only the marrow spaces, but also the empty spaces above the limits of the lesion, which was included in the TV of the standardized-predefined ROI. Therefore, we suggest that, perhaps for this parameter, the use of a ROI with this design is not the best option.

The calculation of Tb.Th, Tb.Sp, and Tb.N was based on a sphere-fitting method, where for Tb.Th measurement, the spheres were fitted to the object, and for Tb.Sp, the spheres were fitted to the background (Bouxsein et al. 2010). This justifies the fact that there was a difference in Tb.Sp and not in Tb.Th, as the quantity of the object did not vary between the methods. However, the backgrounds provided by the two ROI definition methods were different and were greater in the predefined method.

Unlike BV/TV, which considers the entire tissue volume (including non-bone), BS/BV only accounts for bone within the ROI (Bouxsein et al. 2010). Since the amount of bone within the ROI was similar for both groups. Therefore, there were no statistically significant differences between the manual and the predefined groups. Higher BS/BV values indicate that the rate of remodeling is increased (Adams et al. 2022). In the present study, any difference between the manual and predefined groups would not make sense, because the same samples were used for both groups.

Tb.Th tended to be thinner in the irradiated bone than in the non-irradiated bone; however, Tb.N and BV/TV tended to be the same, as shown in a recent study (Mendes et al. 2020). In the present study, none of the parameters showed differences between irradiated and non-irradiated bones, confirming that ionizing radiation had limited effects on the already initiated bone repair process. The effects of ionizing radiation on the woven bone would be more substantial in the total period for this bone to become lamellar, followed by the amount of newly formed bone. Irradiation performed four days or more after surgery in rats did not significantly interfere with the bone healing process, even with very high doses of radiation (Arnold et al. 1998), which justifies the absence of statistically significant differences between the irradiated and non-irradiated groups. The acute effects of RT were observed clinically for a few weeks after treatment. Late effects are typically seen after a latent period of six months or more (Sønstevoid, Johannessen, and Stuhr 2015). The 14 days evaluation period in rats is equivalent to 2–3 months in humans, as rats have a four-six times higher metabolic rate than humans (Schultze-Mosgau et al. 2005). These short periods did not allow for complete repair of the lesion, facilitating its identification during microtomographic analysis.

No statistical differences were found in the FD parameter, which is a measure of self-similar surface roughness and an indicator of irregularity and roughness (Gudea and Stefan 2013; Lee and Jasiuk 2014). Changes in FD reflect changes in the trabecular bone, indicating a loss of trabecular connectivity and increased porosity (Irie et al. 2018). In the present study, trabecular parameters did not show statistically significant differences.

It has been established that more precise contouring for cortical and trabecular bone regions can be achieved using the manual method or automated algorithms, which have been developed to reduce working time and avoid operator bias (Bouxsein et al. 2010; Kenney et al. 2022; Hopkinson et al. 2023). In our case, the use of a standardized predefined ROI reduced the operative time. It is important to consider the use of this type of predefined ROI, because the development of automated algorithms is quite challenging and depends mostly on highly specialized human resources in computer programming.

Despite the limitations of the animal model used in this study, such as the physiological differences between humans and rats, the need to use a reduced sample size owing to ethical issues, among other factors, is not recommended for extrapolating the results of this study to humans, especially in relation to the second objective. Clinical trials are needed to complement our results and provide a better understanding of the bone-repair process in humans subjected to RT.

5. Conclusions

In conclusion, the image segmentation process for woven bone analysis using high-resolution methodology yielded distinct microarchitectural findings when employing a manually defined ROI compared with a standardized predefined one. No significant differences were observed in any of the evaluated parameters when IR was considered. Despite being more time-consuming, the segmentation method involving manual delimitation of the ROI should be prioritized whenever feasible.

Authors' Contributions: PITORRO, T.E.A.: Defined the regions of interest, collected the results and measured time consuming, Performed the statistical analysis and data interpretation, drafted the work, read and approved the final version of the manuscript; IRIE, M.S.: Scanned the samples, performed the statistical analysis and data interpretation, read and approved the final version of the manuscript; BITES, C.O.B.: Performed the statistical analysis and data interpretation, drafted the work, read and approved the final version of the manuscript; BARBOSA, G.L.R.: Participated in the conception and design of the study, critically reviewed the work, read and approved the final version of the manuscript; RABELO, G.D.: Critically reviewed the work, read and approved the final version of the manuscript; SOARES, P.B.F.: Participated in the conception and design of the study, critically reviewed the work, read and approved the final version of the manuscript.

Conflicts of Interest: The authors declare no conflicts of interest.

Ethics Approval: This study was approved by the Bioethics Committee for Animal Experimentation (CEUA #093/17) at the Federal University of Uberlândia, Brazil.

Acknowledgments: This study was supported by grants from the Fundação de Amparo à Pesquisa de Minas Gerais (FAPEMIG), the Coordenação de Aperfeiçoamento de Pessoal de Nível Superior – Brasil (CAPES) – Finance Code 001 and Conselho Nacional de Desenvolvimento Científico e Tecnológico (CNPq) – INCT Saúde Oral e Odontologia - Grants n. 406840/2022-9.

References

- ADAMS, G.J., et al. Microarchitecture and Morphology of Bone Tissue over a Wide Range of BV/TV Assessed by Micro-Computed Tomography and Three Different Threshold Backgrounds. *Medical Engineering and Physics*. 2022, **106**(8), 1-9. <https://doi.org/10.1016/j.medengphy.2022.103828>.
- ARNOLD, M., et al. Radiation-Induced Impairment of Bone Healing in the Rat Femur: Effects of Radiation Dose, Sequence and Interval between Surgery and Irradiation. *Radiotherapy and Oncology*. 1998, **48**(3), 259-265. [https://doi.org/10.1016/S0167-8140\(98\)00039-5](https://doi.org/10.1016/S0167-8140(98)00039-5).
- BEITLITUM, I., et al. A Novel Micro-CT Analysis for Evaluating the Regenerative Potential of Bone Augmentation Xenografts in Rabbit Calvarias. *Scientific Reports*. 2024, **14**(1), 1-10. <https://doi.org/10.1038/s41598-024-54313-4>.
- BOUXSEIN, M.L., et al. Guidelines for Assessment of Bone Microstructure in Rodents Using Micro-Computed Tomography. *Journal of Bone and Mineral Research*. 2010, **25**(7), 1468-1286. <https://doi.org/10.1002/jbmr.141>.
- BUIE, H.R., et al. Automatic Segmentation of Cortical and Trabecular Compartments Based on a Dual Threshold Technique for in Vivo Micro-CT Bone Analysis. *Bone*. 2007, **41**(4), 505-515. <https://doi.org/10.1016/j.bone.2007.07.007>.
- CHAVEZ, M.B., et al. Guidelines for Micro-Computed Tomography Analysis of Rodent Dentoalveolar Tissues. *JBMR Plus*. 2021, **5**(3), 1-17. <https://doi.org/10.1002/jbm4.10474>.
- CHRISTIANSEN, B.A. Bone Reports Effect of Micro-Computed Tomography Voxel Size and Segmentation Method on Trabecular Bone Microstructure Measures in Mice. *BONR*. 2016, **27**(5), 136-140. <https://doi.org/10.1016/j.bonr.2016.05.006>.
- CLARK, D.P. and BADEA, C.T. Micro-CT of Rodents: State-of-the-Art and Future Perspectives. *Physica Medica*. 2014, **30**(6): 619-634. <https://doi.org/10.1016/j.ejmp.2014.05.011>.
- DONAUBAUER, A.J., et al. The Influence of Radiation on Bone and Bone Cells—Differential Effects on Osteoclasts and Osteoblasts. *International Journal of Molecular Sciences*. 2020, **21**(17), 1-19. <https://doi.org/10.3390/ijms21176377>.
- GUDEA, A.I. and STEFAN, A.C. Histomorphometric, Fractal and Lacunarity Comparative Analysis of Sheep (*Ovis Aries*), Goat (*Capra Hircus*) and Roe Deer (*Capreolus Capreolus*) Compact Bone Samples. *Folia Morphologica (Poland)*. 2013, **72**(3), 239-248. <https://doi.org/10.5603/FM.2013.0039>.
- HOPKINSON, M., et al. A New Method for Segmentation and Analysis of Bone Callus in Rodent Fracture Models Using Micro-CT. *Journal of Orthopaedic Research*. 2023, **41**(8), 1717-1728. <https://doi.org/10.1002/jor.25507>.
- IRIE, M.S., et al. Use of Micro-Computed Tomography for Bone Evaluation in Dentistry. *Brazilian Dental Journal*. 2018, **29**(3), 227-238. <https://doi.org/10.1590/0103-6440201801979>.

- JIANG, M., et al. Radiotherapy-Induced Bone Deterioration Is Exacerbated in Diabetic Rats Treated with Streptozotocin. *Brazilian Journal of Medical and Biological Research*. 2021, **54**(12), 1-10. <https://doi.org/10.1590/1414-431X2021e11550>.
- KENNEY, H.M., et al. A High-Throughput Semi-Automated Bone Segmentation Workflow for Murine Hindpaw Micro-CT Datasets. *Bone Reports*. 2022, **16**(6), 1-15. <https://doi.org/10.1016/j.bonr.2022.101167>.
- KIM, Y., et al. MicroCT for Scanning and Analysis of Mouse Bones. *Methods in Molecular Biology*. 2021, **2230**, 169-198. https://doi.org/10.1007/978-1-0716-1028-2_11.
- LEE, W. and JASIUK, I. Effects of Freeze-Thaw and Micro-Computed Tomography Irradiation on Structure-Property Relations of Porcine Trabecular Bone. *Journal of Biomechanics*. 2014, **47** (6), 1495-1498. <https://doi.org/10.1016/j.jbiomech.2014.02.022>.
- MANEM, V.S. and TAGHIZADEH-HESARY, F. Advances in Personalized Radiotherapy. *BMC Cancer*. 2024, **24**(1), 3-5. <https://doi.org/10.1186/s12885-024-12317-3>.
- MENDES, E.M., et al. Effects of Ionizing Radiation on Woven Bone: Influence on the Osteocyte Lacunar Network, Collagen Maturation, and Microarchitecture. *Clinical Oral Investigations*. 2020, **24**(8), 2763-2771. <https://doi.org/10.1007/s00784-019-03138-x>.
- NASCIMENTO, E.H.L., et al. Impact of Micro-Computed Tomography Reconstruction Protocols on Bone Microarchitecture Analysis. *Oral Surgery, Oral Medicine, Oral Pathology and Oral Radiology*. 2019, **128**(4), 411-417. <https://doi.org/10.1016/j.oooo.2019.05.001>.
- OLIVEIRA, L., et al. Fractal Analysis of the Mandible Cortical Bone: Correlation among Fractal Dimension Values Obtained by Two Processing Methods from Periapical Radiograph and Micro-Computed Tomography with Cone-Beam Computed Tomography. *Radiation and Environmental Biophysics*. 2023, **62**(4), 511-518. <https://doi.org/10.1007/S00411-023-01045-0>.
- SARI, E.F., et al. General Dentists' Knowledge, Perceptions, and Practices Regarding Oral Potentially Malignant Disorders and Oral Cancer in Indonesia. *Clinical and Experimental Dental Research*. 2024, **10**(1), 1-11. <https://doi.org/10.1002/cre2.807>.
- SCHULTZE-MOSGAU, S., et al. Expression of Bone Morphogenic Protein 2/4, Transforming Growth Factor-B1, and Bone Matrix Protein Expression in Healing Area between Vascular Tibia Grafts and Irradiated Bone - Experimental Model of Osteonecrosis. *International Journal of Radiation Oncology Biology Physics*. 2005, **61**(4), 1189-1196. <https://doi.org/10.1016/j.ijrobp.2004.12.008>.
- SHIM, J., et al. Micro-Computed Tomography Assessment of Bone Structure in Aging Mice. *Scientific Reports*. 2022, **12**(1), 1-16. <https://doi.org/10.1038/s41598-022-11965-4>.
- SØNSTEVOLD, T., JOHANNESSEN, A.C., and STUHR, L. A Rat Model of Radiation Injury in the Mandibular Area. *Radiation Oncology*. 2015, **10**(1), 1-11. <https://doi.org/10.1186/s13014-015-0432-6>.
- SU, D., et al. Dual-Energy Computed Tomography and Micro-Computed Tomography for Assessing Bone Regeneration in a Rabbit Tibia Model. *Scientific Reports*. 2024, **14**(1), 1-9. <https://doi.org/10.1038/s41598-024-56199-8>.
- VÁSÁRHELYI, L., et al. Microcomputed Tomography–Based Characterization of Advanced Materials: A Review. *Materials Today Advances*. 2020, **8**(12), 1-13. <https://doi.org/10.1016/j.mtadv.2020.100084>.
- VIGUET-CARRIN, S., et al. Association between Collagen Cross-Links and Trabecular Microarchitecture Properties of Human Vertebral Bone. *Bone*. 2010, **46**(2), 342-347. <https://doi.org/10.1016/j.bone.2009.10.001>.

Received: 19 September 2024 | **Accepted:** 15 January 2025 | **Published:** 12 February 2025



This is an Open Access article distributed under the terms of the Creative Commons Attribution License, which permits unrestricted use, distribution, and reproduction in any medium, provided the original work is properly cited.